Stable Hairpins with β-Peptides: Route to Tackle Protein−Protein Interactions

Carsten Baldauf* and M. Teresa Pisabarro*

Structural Bioinformatics, Biotechnologiezentrum der TU Dresden, Tatzberg 47-51, D-01307 Dresden, Germany

Received: August 27, 2007; Revised Manuscript Received: March 10, 2008

Experimental and theoretical data demonstrate that sequences of heterochiral $\beta^{2,3}$-amino acids and a turn-inducing β-dipeptide adopt hairpin-like structures in methanol. On the basis of extensive canonical and replica exchange MD simulations, we could transfer these findings to water as the solvent of physiological relevance. We show that rationally designed β-peptides exhibit a higher folding tendency and a more robust hairpin structure formation in water compared with α-peptides. Furthermore, our designed scaffold enables the addition of a wide variety of functions without disrupting the structure. Since hairpins are often involved in protein interactions, the very stable hairpin-like fold of our designed β-peptides might be used as a lead scaffold for the design of molecules that specifically modulate protein−protein interactions. This is demonstrated by application of this concept to the recognition of proline-rich sequences (PRS) by WW domains, an important interaction in cell signaling. We focus on the possibility to imitate the strands 2 and 3 of any WW domain as a minimal motif to recognize their target sequences PPXY. We conclude that rationally designed β-peptide hairpins can serve as scaffolds not only to tackle PPII recognition but also to open up a way to influence a wide variety of protein−protein interactions.

Introduction

Non-natural oligomers folding into stable and distinct secondary structures are often denoted as foldamers.[1] In the past decade, much attention has been paid to synthesis and structural characterization of such compounds.[2–11] Among the numerous structural possibilities, oligomers of homologous amino acids play a key role. Homologation of α-amino acids leads to β-, γ-, and δ-amino acids, which can be oligomerized to β-, γ-, and δ-peptides.[12–17] Hybrid sequences of such building blocks have also been reported.[18–24] These peptides enlarge the chemical space available for peptide ligand design and give the chance to overcome serious shortcomings of receptor-targeting peptides. Many of these scaffolds show a folding behavior comparable to their native counterparts with the chance to selectively emphasize distinct folds and a better bioavailability due to their stability against proteases.[25,26] Besides the interesting perspectives for drug and nanostructure design, diagnostic agents, and catalysts, these compounds might serve as a benchmark to test our current comprehension of structure formation in biological macromolecules.[27]

At present, oligomers of β-amino acids (β-peptides) are the best understood class of homologous peptides. The distinct secondary structure formation in β-peptides offers ways to imitate α-peptide secondary structure elements and to obtain completely new folds.[12–14,28–32] In particular, helix formation in β-peptides has been intensively investigated.[32–42] Considerable importance comes from the fact that some of the peptidic foldamers exhibit biological activity, as for instance antiviral, antibacterial, and antifungal properties.[43–47] Another important point is the inhibition or modulation of protein−protein interactions with β-peptides[48–51] or α/β-hybridpeptides.[52,53]

Protein−protein recognition does not need to necessarily be tackled with non-natural helical structures. The use of hairpin-like structures could be another promising way, as β-hairpins are secondary structural motifs often found in protein recognition and, therefore, are of great pharmacological interest. A very interesting and representative example of cell signaling protein−protein interactions is the recognition of proline-rich sequences (PRS) by WW domains, the smallest polyproline II (PPII) fold recognizing domain.[54] The WW domain consists of about 40 residues that form a three stranded β-sheet.[55–59] The human Yes associated protein YAP65 exhibits a type I WW domain and recognizes the sequence motif PPXY in a PPII fold. Data from structural investigations suggest that only the strands 2 and 3 of YAP65 WW are involved in recognition of the target sequence.[59,60] This suggests the possible reduction of the WW domain to a β-hairpin consisting of two hydrogen-bonded β-strands linked by a turn. A recent attempt to design and autonomously fold a β-hairpin composed of α-amino acids to prove strands 2 and 3 of the WW domain as the minimal PPII binding motif has failed.[61] The necessary compromise between obtaining a stable fold and, at the same time, obtaining the desired function was possibly a too strong limitation. Only a subset of α-amino acid building blocks enforces folding toward hairpin structures, a fact which limits the available functionalities significantly.[62,63] Additionally, there are general shortcomings of α-peptides, including their sensitivity against proteases and their limited affinity and selectivity.[64]

Therefore, we want to explore the use of β-peptide hairpins as scaffolds to tackle protein−protein interactions. It is known that oligomers of heterochiral $\beta^{2,3}$-amino acids (Figure 1a) form extended strand-like structures.[13,65–67] This effect is due to the steric demand of the vicinal substituents at the C_α and C_β positions of the β-amino acid building blocks, which locks the central torsion in a *s*-trans conformation (Figure 1b). The structure formation in β-peptides and the higher homologues depends, disregarding solvent influence, more on the position

* Corresponding authors. Phone: +49 351 463 400 77. Fax: +49 351 463 400 87. E-mail: carsten@picb.ac.cn (C.B.); mayte.pisabarro@biotec.tu-dresden.de (M.T.P.).

10.1021/jp076838r CCC: $40.75
Published on Web 05/30/2008

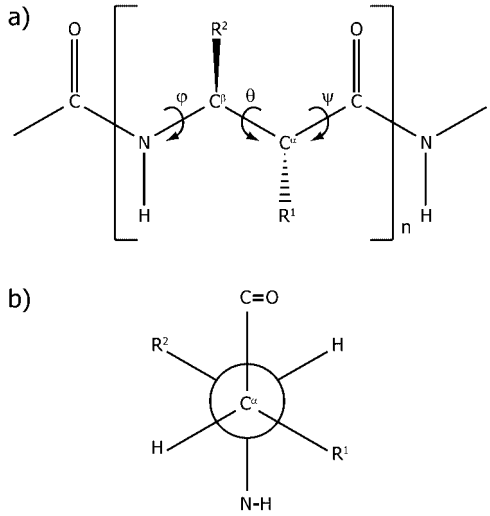

Figure 1. (a) Heterochiral $\beta^{2,3}$-amino acid oligomer; (b) Newman projection of a β-amino acid building block along the central torsion angle θ.

and stereochemistry of the substituents than on their chemical nature or size.[13,14] Studies on a β-peptide consisting of a turn motif and two strand-like sequences published by Seebach and co-workers[65] indicate a strong tendency toward the formation of hairpin-like structures. The major differences between β-hairpins in native proteins and β-peptide hairpins are (i) β-hairpins are slightly twisted around their length axis and β-peptide hairpins are not; (ii) β-peptide hairpins form all H-bonds in the same direction relative to the sequence; (iii) each residue in a β-peptide hairpin presents one side chain to every face of the hairpin, whereas the side chains of the residues in β-hairpins point alternating to the one or the other side.

Small, but independent folding peptides are of great interest to target protein−protein interactions. These interactions are important for many biological functions, for instance, the mediation of signals through the cell in signaling pathways or the aggregation of large enzyme complexes. However, the handling of their interactions and the selective modulation of their interfaces is a great challenge. The extremely large interacting areas ranging from 10 up to almost 100 nm^2 and the promiscuity of interactions due to the hegemony of unspecific hydrophobic effects limit the use of small molecules as modulators of protein interactions.[68]

We employ replica exchange molecular dynamics (REMD) simulations[69−72] in our study on the folding behavior of several designed β-peptide hairpins in water and suggest these β-peptides as a scaffold for a specific modulation of protein−protein interactions.

Methodology

We studied a series of β-peptide hairpins to develop the peptides HP1, HP2, and HP3 (cf. Figure 2). Sequences of the peptide models can be found in Table 1. The layout of these designed molecular scaffolds considers two aspects, the designated functions to achieve binding affinity and specificity (A-side; cf. Figure 2) and the interacting residues to stabilize hairpin formation (B-side; cf. Figure 2). The central dipeptide (residues 5 and 6, BGV-BKG), known to act as a turn-inducing sequence,[65] is crucial for the formation of a hairpin-like structure. Stabilization of the hairpin is intended by π−cation interaction between the Tyr side chain of residue 2 and the Arg side chain of residue 9, and by the hydrophobic packing between the aliphatic side chains of residue 3 and and those of residue 8. The two Trp side chains on side A (cf. Figure 2) that introduce specificity and affinity by forming a wall of the Pro-Pro recognition pocket should also stabilize the fold through π interactions. The β^3-positions of residues 2 to 4 and the β^2-position of residues 7 to 9 are free for substitutions with side chains of virtually any function and chemistry. The range of possible side chains is only limited by synthetic availability and not to the canonical functionalities of the α-peptides. Thus, the availability of possible functions and binding sites is enormous to allow side chains and functionalities to be adapted to virtually any need.

The structural properties of the β-peptide scaffolds were compared to two representative α-peptides: (i) G4, an α-peptide designed to form a hairpin and to resemble the binding site of the YAP65 WW domain;[61] and (ii) Trpzip2, a Tryptophan zipper hairpin of known stable fold (PDB: 1LE1).[73−75] Their sequences can be found in Table 1.

All simulations and part of the analysis were carried out with the Gromacs suite of programs (version 3.3.1).[76,77] The Gromos 96 (53a6) force field[78,79] has proven to work well also for β-amino acids and β-peptides.[65,80−83] We had to extend the Gromacs-topologies of the Gromos force field to selected β-amino acids, which are available from the authors upon request. The necessary amount of counterions (Cl^- and Na^+) was added to ensure a neutral system. Previous to the productive MD simulations, steepest descent energy minimizations and position restrained MD simulations to energy convergence (20 to 100 ps) were performed. The protonation state of the peptide was assumed for pH 7. We studied the folding behavior of the α- and β-peptides unbiased from previous structural investigations. The starting conformations were completely extended in all simulations and at all different simulation temperatures. VMD[84] and POV-Ray were used for visualization.

The canonical MD-simulations were performed with a standard setup for 10 ns. The molecules were solvated in a large dodecahedric box containing about 14 000 SPC water molecules. Thereby, a minimum distance of 1.5 nm between the fully extended solute and the box borders was assured. Periodic boundary conditions were applied. The temperature (298 K) and pressure (1 bar) were weakly coupled following the Berendsen method with time constants of 0.1 and 0.5 ps, respectively.[85] Coulomb and van der Waals interactions were modeled with a twin range cutoff (0.8 and 1.4 nm). Constraints were applied with the SHAKE algorithm.[86]

One limitation of classical MD techniques in the description of the folding behavior of peptides and proteins is the poor sampling of the available conformational space. The system has a tendency to get trapped in local minima instead of reaching the thermodynamically most stable state. REMD simulations[69−72] offer the possibility to overcome this shortcoming. Because of the parallel simulation at different temperatures and the frequent exchange of conformations (replicas) between them, an enhanced sampling of the conformational space is ensured. To obtain deeper insight into the folding properties of the β-peptide hairpins and in order to compare with α-peptides, replica exchange MD (REMD)[69,71] simulations at constant pressure (NPT)[72] were performed for HP2, G4, and Trpzip2 (cf. Table 1). The completely extended peptides with all backbone torsion angles set to 180° (with exception of the D-Pro residue of G4) were centered in small dodecahedric boxes of SPC water molecules. Since the exchange probabilities are based on a Metropolis criterion employing the differences in temperature and potential energies of two replicas, the exchange rate depends

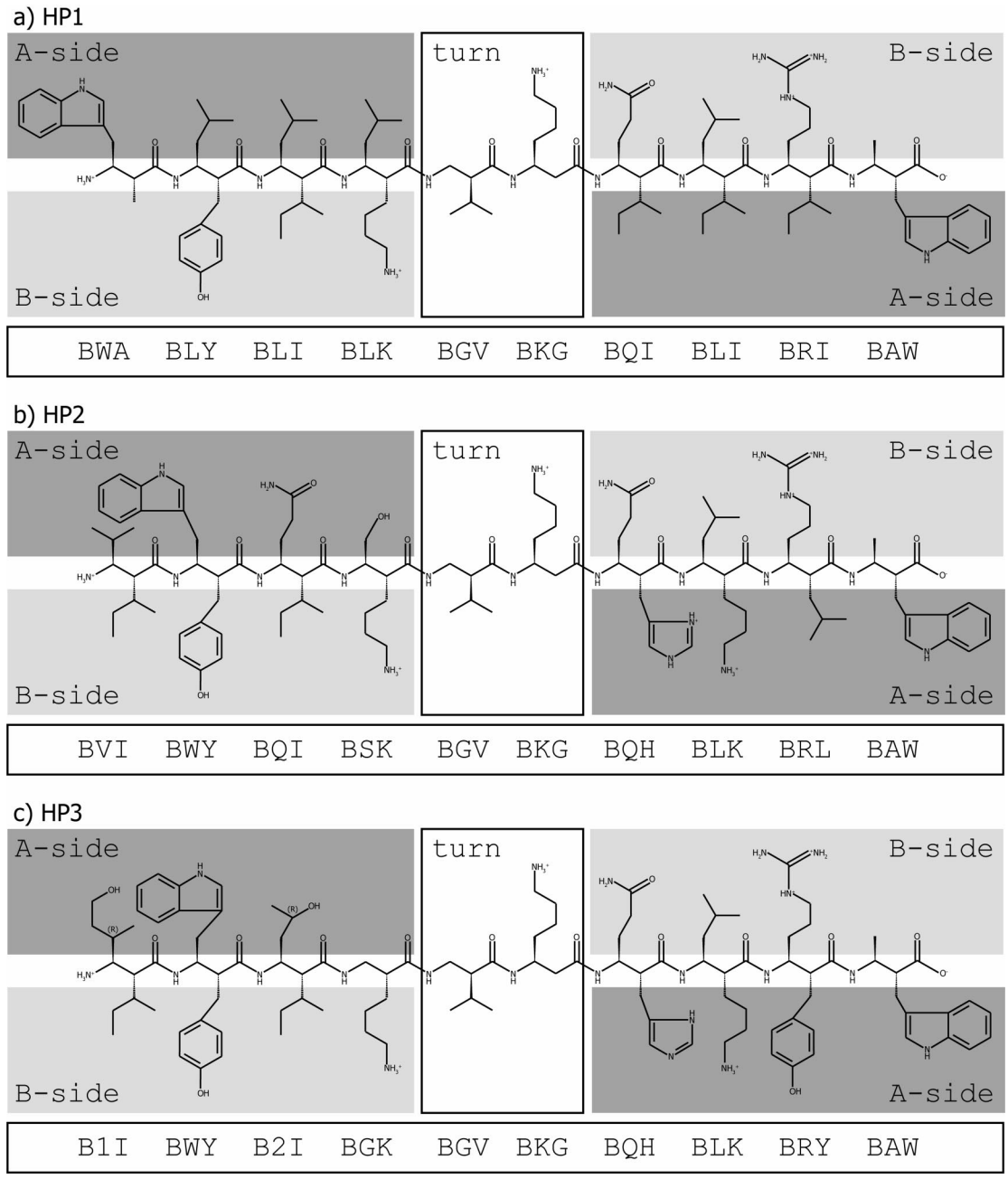

Figure 2. Studied β-peptide hairpins HP1 (a), HP2 (b), and HP3 (c) consist of three main elements, the turn region and the sides A and B. Refer to Table 1 for the three letter codes.

TABLE 1: Peptide Sequences in This Study

name	sequence
α-Peptides	
G4[a]	RYFLNHVpGKQTTTWQ-NH_2
Trpzip2	SWTWENGKWTWK-NH_2
PP2	GTPPPPYTVG
β-Peptides[b]	
HP1	BWA-BLY-BLI-BLK-BGV-BKG-BQI-BLI-BRI-BAW
HP2	BVI-BWY-BQI-BSK-BGV-BKG-BQH-BLK-BRL-BAW
HP3	B1I-BWY-B2I-BGK-BGV-BKG-BQH-BLK-BRY-BAW

[a] The lower case "p" stands for D-Proline. [b] The three letter code for the β-amino acids: 1st letter: B means β-amino acid; 2nd and 3rd letter: Side chain of the corresponding α-amino acid placed on the Cβ- or Cα-atom, respectively. Numbers correspond to non-natural side chains, cf. Figure 2 for chemical structures.

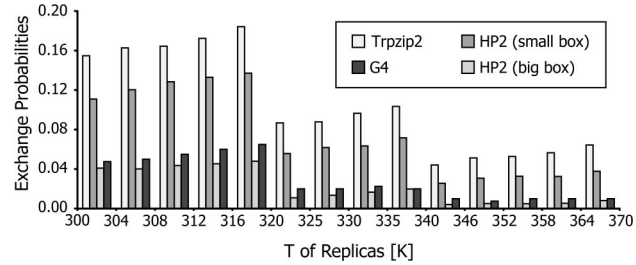

Figure 3. Exchange probabilities between the different replicas for the simulations of Trpzip2, HP2, and G4.

on the system size. Thus, it is crucial for comparability to use similar sized systems and the same temperatures for the replicas.

In the first trials, we tried to reduce computation time by using tailored water boxes for each system. Because of the length of the extended peptides, we have chosen dodecahedric boxes with an image distance of 5.7, 5.0, and 4.5 nm for the peptides G4, HP2, and Trpzip2, respectively. This results in significantly

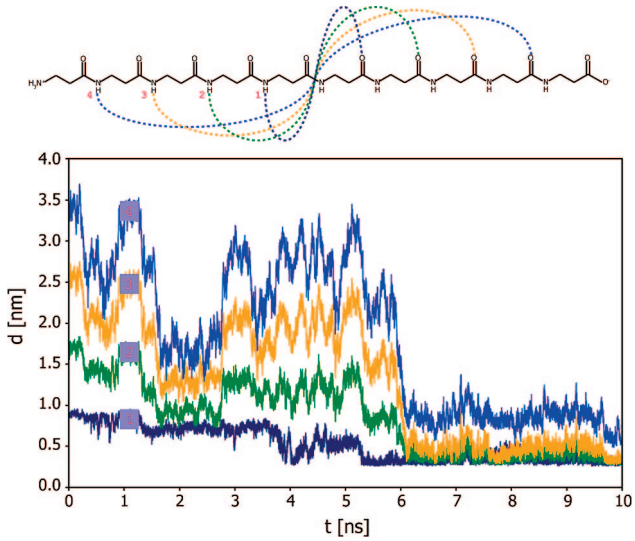

Figure 4. Plot of the H-bond distances monitored during the simulation time of a 10 ns trajectory of HP1 starting from a fully extended conformation.

different exchange rates (exchange rates for Trpzip2, HP2 (small box), and G4 in Figure 3) and thus falsifies the comparison of populated structures. To overcome this issue and to ensure a good comparability of our β-peptide to the strongly related α-peptide G4, we recalculated the 20 ns trajectory of HP2 (big box) in a box of the same size as for G4. The very similar exchange rates obtained (cf. Figure 3) allow direct comparison of the folding properties from the sampling trajectory at 300 K, which is a goal of this study. For the REMD, 15 replicas with temperatures of 300, 304, 308, 312, 316, 320, 325, 330, 335, 340, 346, 352, 358, 364, and 370 K were used. A simulation at 380 K was not part of the REMD setup but was used for comparisons. The simulations were carried out for 20 ns, meaning an overall 300 ns sampling time for each peptide obtained by the parallel simulation of 15 replicas. A twin range cutoff for van der Waals (0.9/1.4 nm) and a smooth particle mesh Ewald algorithm for Coulomb interactions (switching distance of 0.9 nm) were used. The neighbor lists were updated every 0.01 ps.[87] Temperature and pressure were kept constant by Berendsen weak coupling[85] with coupling constants of 0.1 ps for the temperature and 1 ps for the pressure. Constraints were applied to the bonds of the peptide with the LINCS algorithm.[88] To analyze the results of the REMD simulations, the conformations of the lowest temperature trajectories were clustered by a simple rmsd criterion for the backbone atoms (C, Cα, N, O, and in case of the β-peptide Cβ additionally, rmsd cutoff 0.1 nm) of the last 15 ns of the sampling trajectories at 300 K, and the development of distances of selected backbone atoms were measured.

The REMD simulations for the β-peptide hairpin HP2 were extended to 40 ns for each of the 15 replicas, resulting in an overall sampling time of 600 ns. In order to identify the native state, we computed Gibbs free energy landscapes with respect to different properties. Potentials of mean force (PMF) were generated on the basis of histograms of measured properties of the β-peptide HP2 from the 40 ns REMD trajectories. One-dimensional histograms were generated from rmsd values to an idealized hairpin and from means of measured H-bond distances corresponding to the desired hairpin structures. These properties were portioned in bins with a width of 0.1 or 0.01 nm, respectively. Two dimensional (2D) histograms were generated with the means of two sets of intramolecular distances

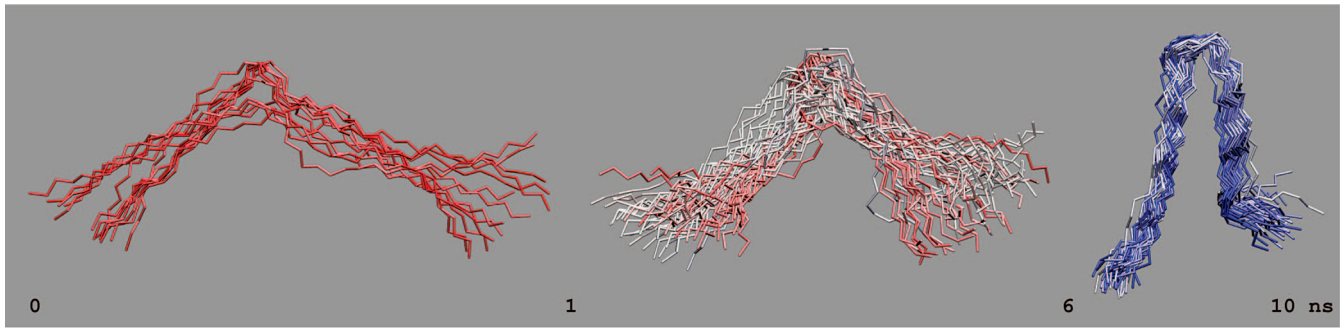

Figure 5. Ensemble of structures from the initial 10 ns trajectory of the β-peptide HP1 showing the folding from the extended to the hairpin-like conformation.

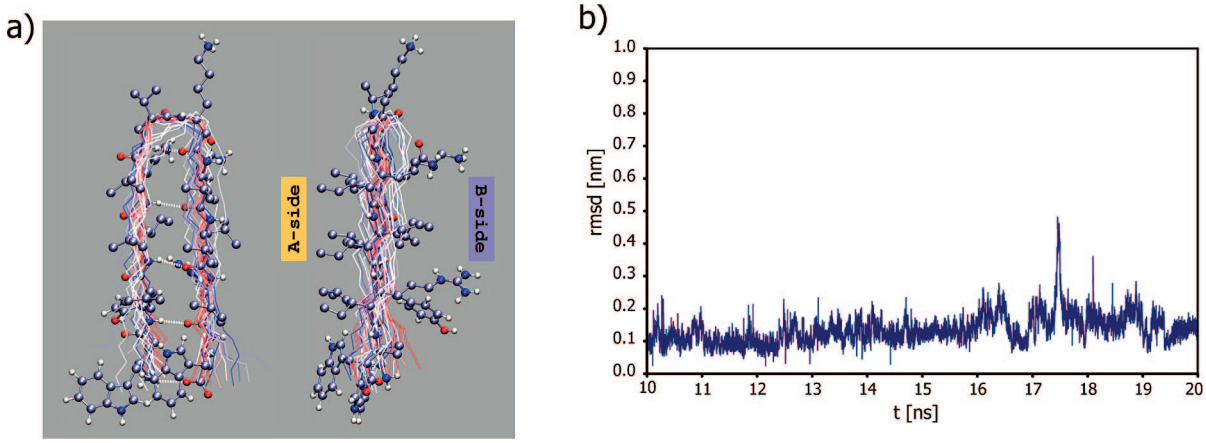

Figure 6. Last 10 ns from a 20 ns trajectory of HP1: (a) ensemble of structures; (b) rmsd plot for the backbone atoms (N, C$^{\beta}$, C$^{\alpha}$, C).

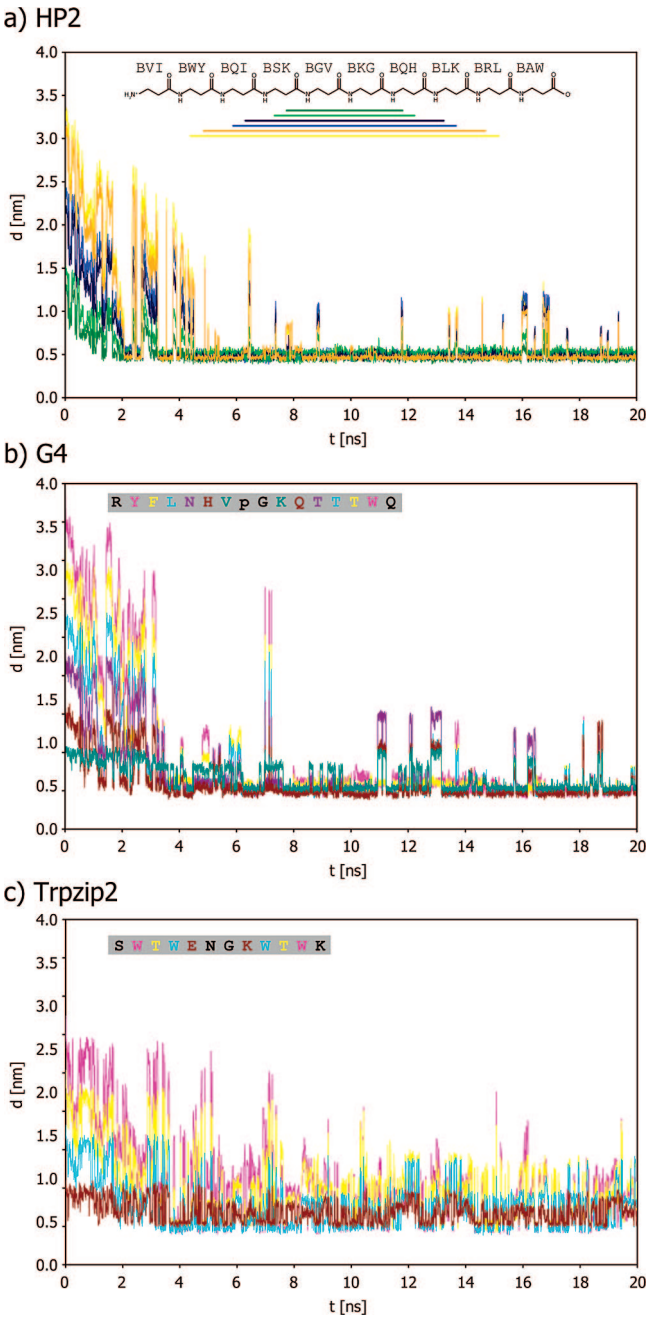

Figure 7. Monitoring the distances between backbone carbons (Cα···Cβ or Cα···Cα, respectively) during the 20 ns REMD simulation of (a) HP2, (b) G4, and (c) Trpzip2. Only the data for the respective replicas at 300 K is shown. The lines are colored as indicated with the lines under the formula or in the single letter code sequences.

corresponding to the two mainly populated folding alternatives as reduced coordinates. Each of these distance means was partitioned in 30 bins with a width of 0.05 nm yielding a 2D histogram of 25 × 25 bins. The Gibbs energy of a bin (x, y) is then given by the probability $P(x, y)$ with respect to the global minimum P_{min} following the general equation:

$$\Delta G(x,y) = -k_B T \ln \frac{P(x,y)}{P_{min}} \quad (1)$$

Results and Discussion

The β-peptide HP1 is our proof-of-concept, that hairpin formation of rationally designed β-peptides takes place in water. Our scaffold folds within only 6 ns from extended state to a

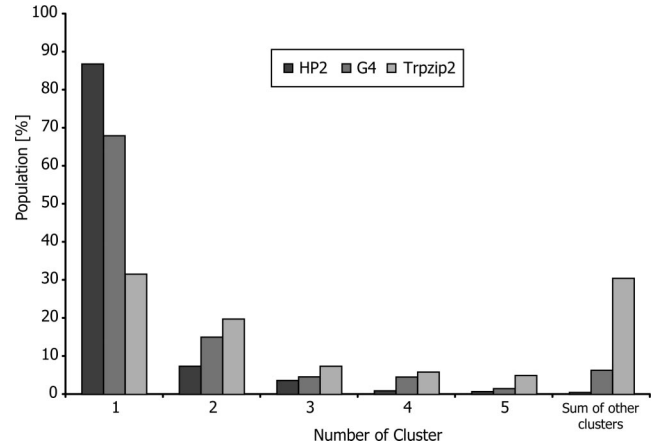

Figure 8. Population after rmsd clustering with 0.1 nm cutoff of the 300 K sampling trajectory from 5 to 20 ns. There are 7 clusters for HP2, 19 clusters for G4, and 60 clusters for Trpzip2. Only the five highest populated clusters are shown in detail, the rest are summed up.

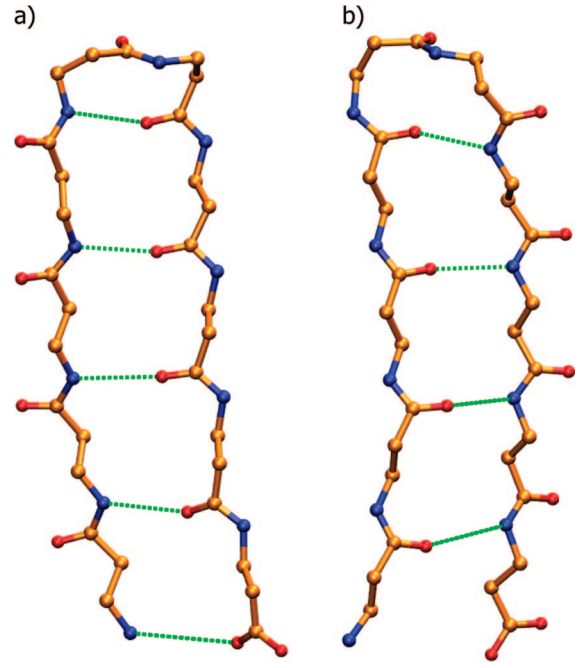

Figure 9. Representatives of the two highest populated clusters from the REMD simulations of HP2: (a) Conformer C_{10}, the "productive" conformation, with a 1 → 2 turn (cluster 1 from Figure 8); (b) Conformer C_{12} with a 1 ← 4 turn (cluster 2 from Figure 8).

hairpin-like structure and remains stable as such in a 10 ns canonical MD simulation (cf. Figure 4). The folding process occurs in a zipper-like manner nucleated at the turn region (residues 5 and 6), and closing the hydrogen bonds step-by-step toward the termini (cf. Figure 5). From the formation of the hairpin-like structure at 6 ns simulation and also after extension of the simulation to 20 ns, the conformation does not change and remains stable (cf. Figure 4 and 6). Only the terminal residues show certain flexibility (cf. Figure 5). The adopted conformation of the β-peptide HP1 resembles data obtained experimentally and computationally in methanol for a similar less hydrophilic β-peptide hairpin.[65] The averaged torsion angles of the strand-like residues 1 to 4 and 6 to 10 ($\varphi = -120°$, $\theta = -175°$, $\psi = 135°$) are in perfect agreement with data obtained by ab initio MO theory calculations on blocked heterochiral

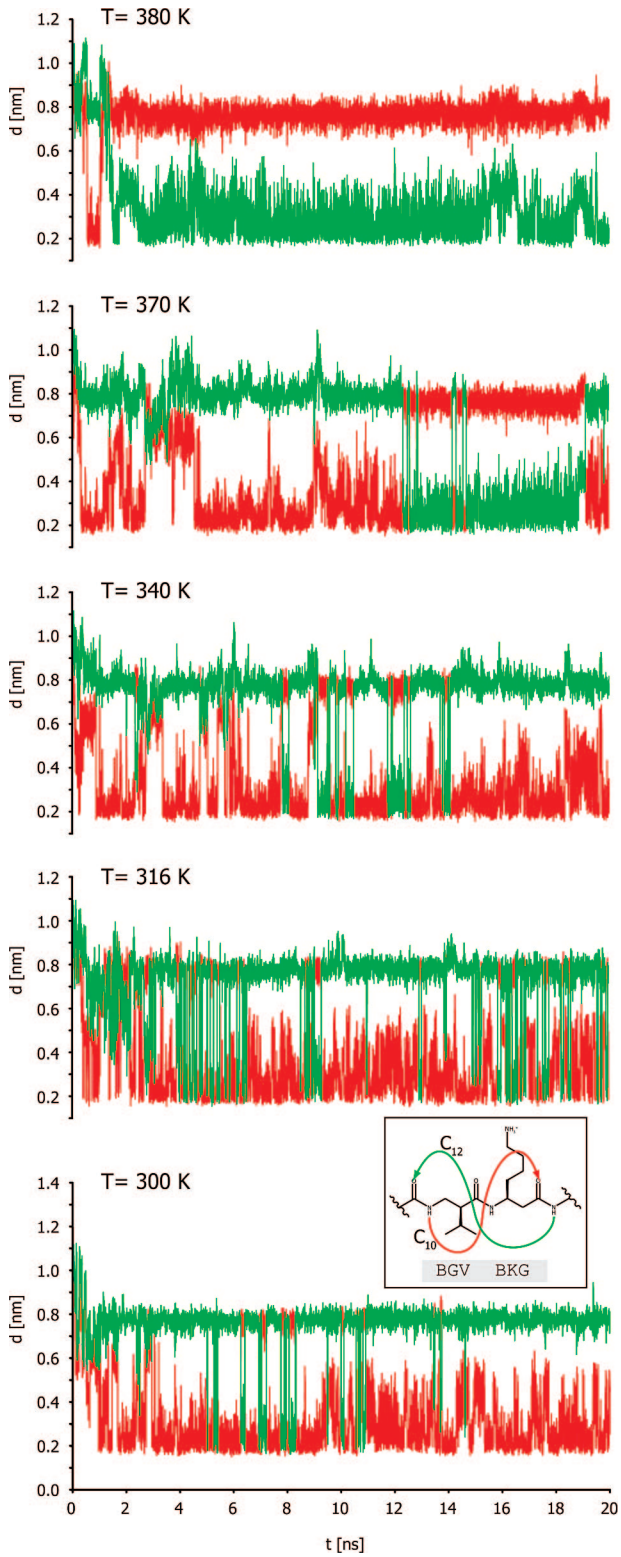

Figure 10. Distances (N−H···O═C) of the two H-bond alternatives C_{10} (1 → 2, red) and C_{12} (1 ← 4, green) in the turns of the two highest populated clusters monitored during the 20 ns of REMD for different temperatures. Colors refer to the scheme. Distances around 0.2 nm suggest H-bond formation and thus population of the C_{10} (red) or C_{12} (green) conformer.

$\beta^{2,3}$-amino acids.[13,66] In employing the same MD approach on G4, no folding event toward a β-hairpin was monitored (data not shown).

The prototype-peptide HP2 presents polar side chains on side A (Figure 2b) instead of the mostly aliphatic side chains on the A-side of HP1. Thus, we can prove that the hairpin formation in these β-peptides is not like a hydrophobic collapse induced by side chain hydrophobicity. HP2 combines the functionalities of HP1 that lead to rapid and robust formation of hairpin-like folds (cf. Figure 2a and 2b) with our first attempts to mimic the PRS binding site of the WW domain. The REMD simulations are intended to prove the results from the MD simulations of HP1 and to provide comparability to the folding behavior and conformational stability between HP2 and the two α-peptide hairpins (G4 and Trpzip2). HP2 shows again the strong folding tendency toward a hairpin-like conformation. Because of the enhanced sampling of REMD with trajectories at higher temperatures (up to 370 K), the sampling trajectory at 300 K pays a first visit to the hairpin-like conformation already after 2 ns simulation time. A distance of approximately 0.5 nm between all respective backbone carbon atoms means a parallel orientation of the residues 1 to 4 and 7 to 10 and thus a hairpin-like conformation (cf. Figure 7a). Once the hairpin is formed, it remains stable for the rest of the simulation time. The conformational features of HP2 are similar to the ones of HP1 discussed above. Because of the reduced side chain hydrophobicity of HP2, we conclude that the stability of the hairpin-like conformation results from three points: (i) backbone hydrophobicity, (ii) the conformational lock of the central torsion due to the heterochiral substituents at Cα and Cβ, leading to the strand-like structures, and (iii) the tendency of the central motif to form a turn conformation. Our results agree well with published data from theoretical and experimental investigations on a comparable system in methanol.[65] The slight noise (peaks of the graphs in Figure 7a) is inherent to this method and represents an exchange of replicas, in this case between the 300 K and the 304 K trajectories. The observation of the contiguous replicas shows a comparable behavior, while for higher temperatures a folding alternative begins to populate more. The clustering of the 300 K trajectory from 5 to 20 ns with an rmsd cutoff of 0.1 nm results in 7 different clusters (Figure 8). Conformer C_{10} is populated at a rate of around 87%, and the competing conformer C_{12} is populated at a rate of 7%. There are nearly no folding alternatives, and the observed flexibility results from the turn segment.

In conformer C_{10}, the central turn forms a hydrogen bond in the forward direction along the sequence (from the NH of residue 5 to the CO of residue 6, 1 → 2 interaction) closing a 10-membered pseudocycle (cf. Figure 9a). The alternative conformer C_{12} is characterized by a 12-membered pseudocycle and a hydrogen bond from the NH of residue 7 to the CO of residue 4 (cf. Figure 9b). This turn conformation shows a 1 ← 4 interaction and is thus a β-peptide variant of an α-peptide β-turn. The conformation of the turn influences the H-bond orientation of the whole hairpin. The C_{12} conformer features only H-bonds in the backward direction, while conformer C_{10} features only H-bonds in the forward direction. The conformer C_{12} is nevertheless barely populated or absent in the trajectories with lower temperature (cf. Figure 10). The importance of conformer C_{12} rises only with the temperature, being the highest populated fold during the simulation time of the unphysical trajectory at 380 K. In the sampling trajectory at 300 K, only the conformer C_{10} is found in a considerable amount, with only few alternative folds. This competition between turn conformations with H-bonds in the forward direction and those in the backward direction is not known from α-peptides. Local H-bonding in α-peptides, as in turns and helices, features only H-bonds in the backward direction along the sequence. In contrast, β-peptides and the higher homologues are known to

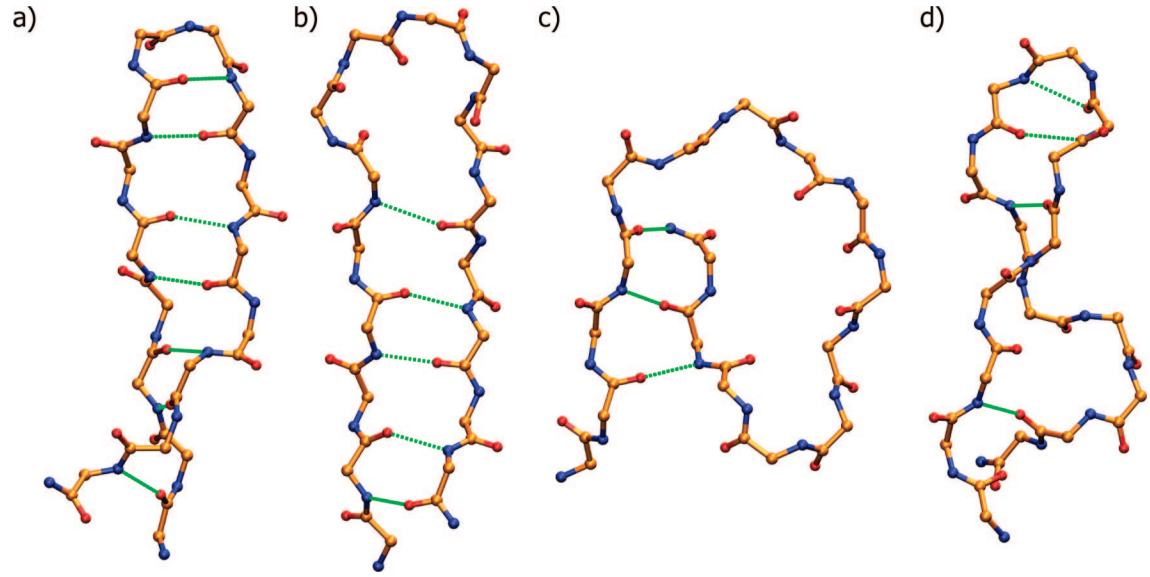

Figure 11. Representative snapshots from the 300 K trajectory of G4: (a) "productive" hairpin conformation (cluster 1, Figure 8); (b) "mismatched" hairpin (cluster 2, Figure 8); (c) "curled" conformer (cluster 3, Figure 8); (d) "mismatched" hairpin with a γ-type turn around the D-Pro (cluster 4, Figure 8).

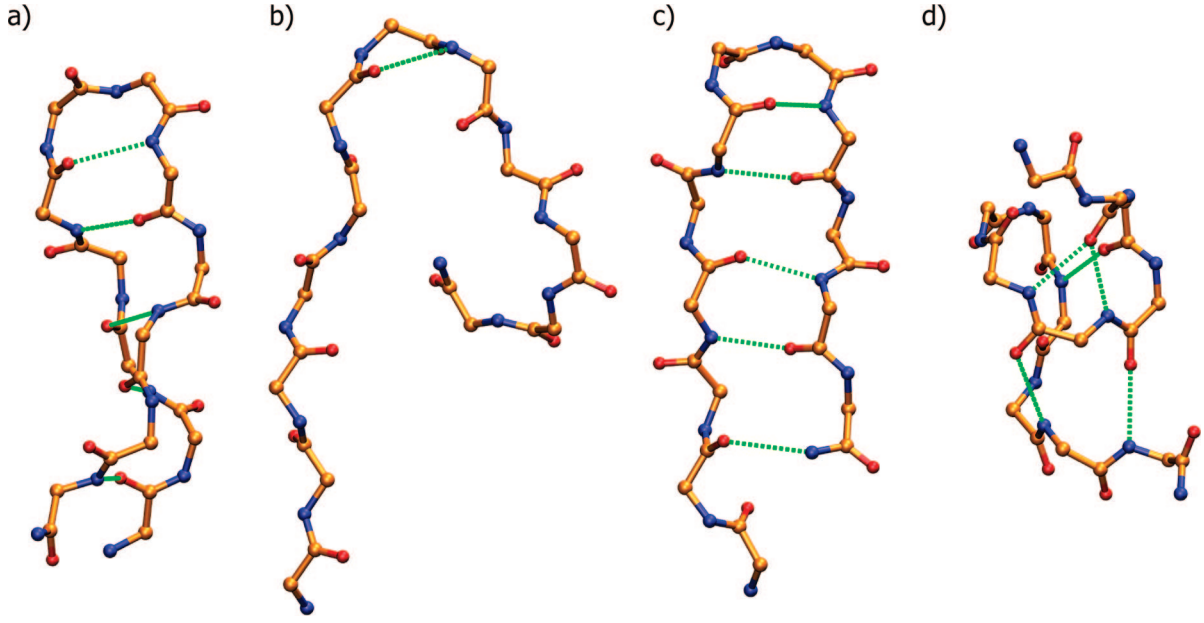

Figure 12. Representative snapshots from the 300 K trajectory of Trpzip2: (a) "productive" hairpin conformation (cluster 1, Figure 8); (b) no hairpin, γ-turn at the Gly residue (cluster 2, Figure 8); (c) "mismatched" hairpin (cluster 3, Figure 8); (d) distorted helical conformation (cluster 4, Figure 8).

form also local H-bonds in the forward direction.[14] The two most frequently found helical conformations in β-peptides are the H_{14}-helix[29–31,89] based on $1 \rightarrow 3$ interactions in the forward direction and the H_{12}-helix[33,90] based on $1 \leftarrow 4$ interactions in the backward direction.[32]

The first appearance of a β-hairpin in the simulation of the α-peptide G4 takes place after 4 ns. This is shown in Figure 7b with the monitoring of the distances between the corresponding Cα atoms. There are more drastic structural fluctuations and more alternative folds for G4 than for HP2. Nevertheless, the highest populated conformation among the 18 alternatives (clustering by rmsd with a 0.1 nm cutoff; only 7 for HP2) is the desired β-hairpin (Figures 8 and 11a) with a proportion of about 67%. The β-hairpin conformation (cluster 1, Figure 11a) includes the formation of sheet-like conformation in the residues 1 to 7 and 10 to 16, while the dipeptide D-Pro-Gly forms a βII′-turn with torsions of $\varphi_2 = 68°$, $\psi_2 = -105°$ and $\varphi_3 = -115°$, $\psi_3 = 12°$. This is in perfect agreement with data from ab initio calculations (HF/6−31G*) predicting angles of $\varphi_2 = 64.2°$, $\psi_2 = -131.4°$ and $\varphi_3 = -96.3°$, $\psi_3 = 10.5°$.[91] Alternative folds are mismatched hairpins with non-β-turns represented by, for example, cluster 2 with a small loop (cf. Figure 11b) and cluster 4, a distorted hairpin with a γ-turn at the D-Pro residue (cf. Figure 11d). Additionally there is a "curled" conformation (cluster 3, Figure 11c).

G4 was designed to mimic the PRS binding region of the YAP65 WW domain. Previous investigations on this peptide included structural investigation with NMR and binding studies to a PPII peptide (PP2, Table 1).[61] However, no binding between this peptide ligand and the hairpin G4 was observed. Nevertheless, the assumption that the PRS binding region of the WW domain can be reduced to the strands 2 and 3 is not necessarily

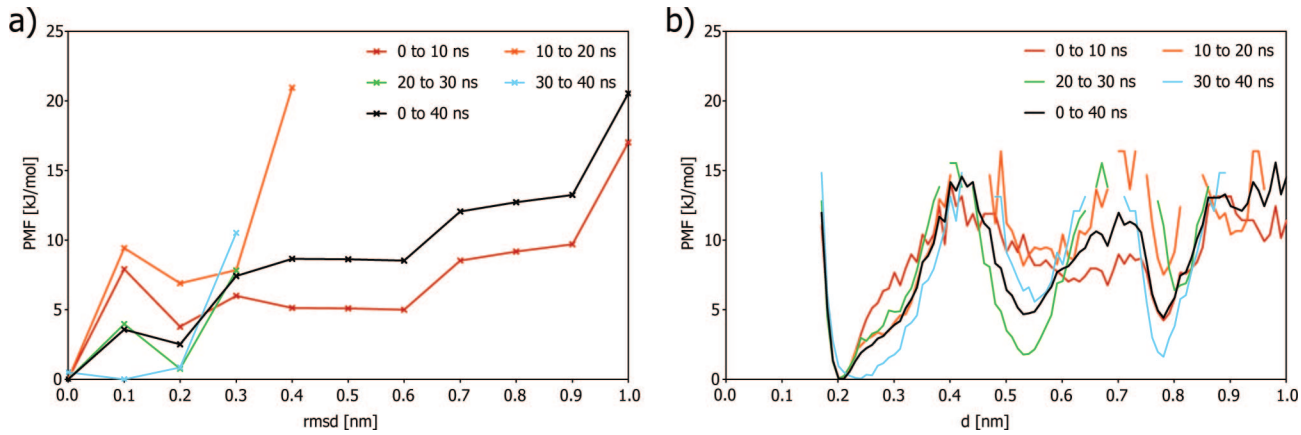

Figure 13. PMF plots for selected time frames of the 300 K replica of HP2. The reduced coordinate in graph (a) is the rmsd to an idealized β-peptide hairpin of type C_{10}; in (b) the reduced coordinate is the mean of the H-bond distances of C_{10}.

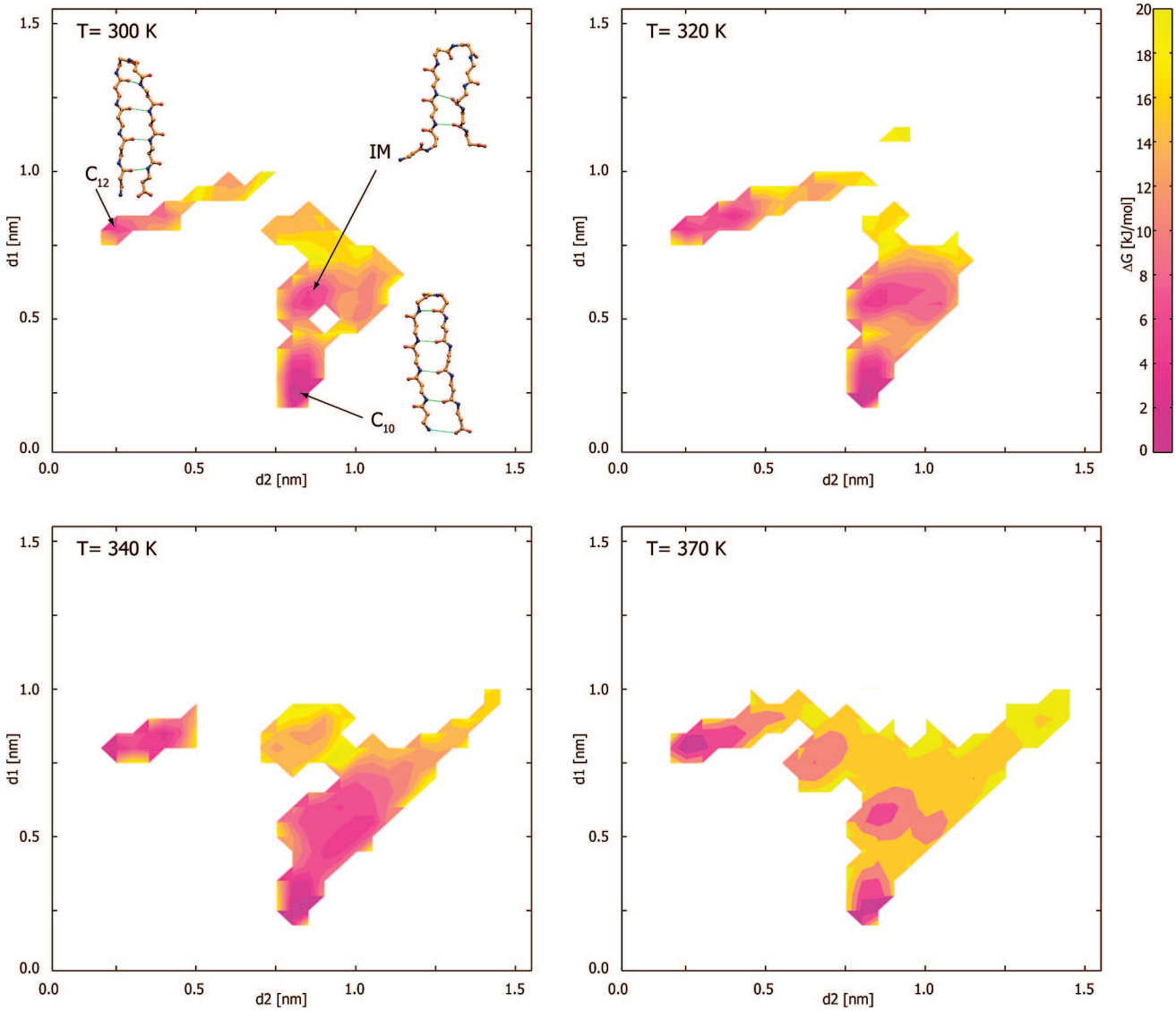

Figure 14. PMF plots of HP2 at 4 different temperatures were derived from 2D histograms of the intramolecular distance means d1 and d2.

wrong. The hydrophobic patch bordered by the large aromatic residues Tyr28 and Trp39 of the YAP65-WW is of great importance for the binding to PRS. In G4, the respective residues Tyr2 and Trp15 are in close proximity to the termini, and thus the high flexibility of these regions probably prevents the formation of the necessary conformation for binding.

Trpzip2 is intended as another benchmark for comparison with the folding behavior of HP2. A constant convergence of the Cα distances monitored in Figure 7c can not be observed. The formation of a hairpin structure in Trpzip2 seems not as favored as for the two previous peptides HP2 and G4. This is partially due to the relatively small system size and the resulting

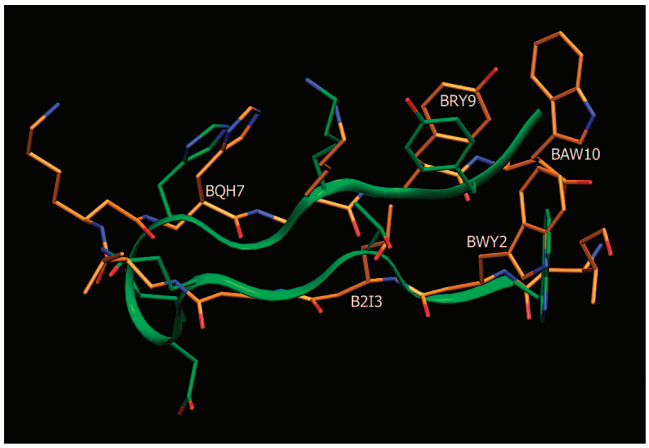

Figure 15. Comparison between the strands 2 and 3 of the YAP65 WW domain (residues 27 to 39, green carbon atoms and ribbon, from PDB 1JMQ) and HP3 (orange carbon atoms). Only side chains of YAP65-WW pointing towards the PPII ligand and a backbone ribbon are shown.

high exchange probabilities (Figure 3). Nevertheless, the large accessible conformational space for Trpzip2 with its 60 independent conformers (cf. Figure 8) renders clearly the enormous flexibility, especially in comparison to HP2. The highest populated cluster (just 30%) has an rmsd of only 0.088 nm referred to the lowest energy model from the PDB entry 1LE1.[73,74] Alternatively, there are mismatched hairpins with either γ-turns (cluster 2) or β-turns formed by other residues than 5 to 8 as in the original structure. Even helical conformations can be observed, for example, in cluster 4. Representative examples for the four highest populated clusters are illustrated in Figure 12.

Our results show the strong tendency of our designed β-peptides to form hairpin-like structures, especially in comparison with α-peptides of similar size. The simulations of HP2 show its robust folding tendency toward a hairpin-like conformation and also its ability to carry functions on one face to obtain affinity and specificity toward other molecules. Summarizing, our data clearly show that, in contrast to G4 and Trpzip2, HP2 has no alternative folds to hairpin-like conformations.

Gibbs Free Energy Landscapes of HP2. To get a clearer view of the folding properties of HP2 and to ensure the convergence of our simulations, we estimated free energy landscapes at 300 K (cf. Figure 13a) with respect to the backbone rmsd to conformer C_{10} (cf. Figure 9a). We see convergence of the simulation toward equilibrium of the two folding alternatives already shown in Figure 9. The global minimum with an rmsd between 0.0 and 0.1 refers mainly to conformer C_{10}. The second, less populated, and therewith energetically less favored minimum corresponds to conformer C_{12} (rmsd 0.2 nm).

An alternative reduced coordinate, promising a better resolution to differentiate the main conformers and to monitor the transition, is the mean of H-bond distances as shown for conformer C_{10}. The resulting PMF plot in Figure 13b features three minima. The native state at 300 K is C_{10} with a d value of approximately 0.2 nm. For conformer C_{12}, the mean distance adopts a value of around 0.8 nm. A third minimum can be found at about 0.5 nm, which is an intermediate (IM) in the transition between C_{10} and C_{12} that features only two H-bonds and presents the central turn opened. The comparison of the rmsd-based versus the distance mean-based PMF reveals the loss of information by breaking down the coordinates to the rmsd value, which is due to the close proximity of the hairpin alternatives C_{10} and C_{12} in the rmsd space.

A more detailed view on the folding landscape and especially on the structural transition between the two conformers can be obtained by comparing the PMF from 2D histograms of replicas at different temperatures (cf. Figure 14). Reduced coordinate d1 is the same as d in Figure 13b, the mean of the H-bond distances of C_{10}, while d2 is the mean of the H-bond distances that refer to conformer C_{12} (cf. Figure 9). The resulting Gibbs free energy landscapes at temperatures 300, 320, 340, and 370

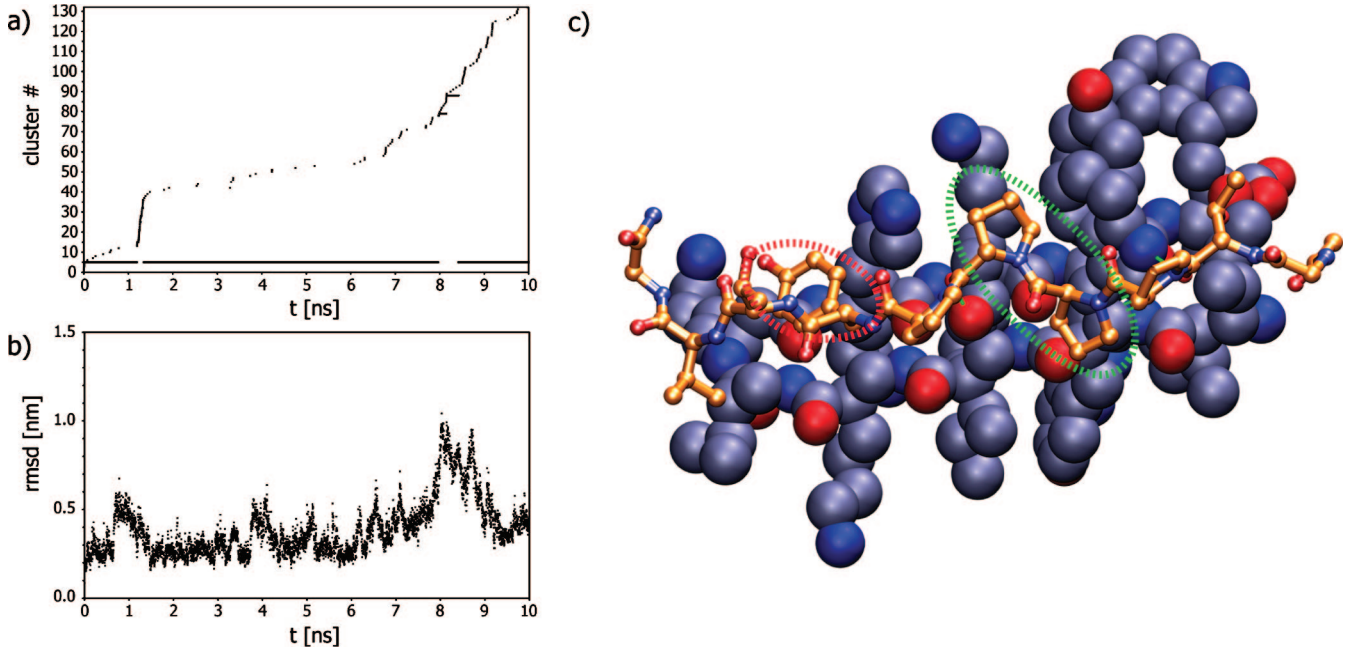

Figure 16. (a) Distribution of the 132 clusters found over the simulation time. (b) Rmsd values of the PPXY motif of PP2 after fitting of the system to the HP3 backbone. (c) "Middle structure" of cluster 5 (cf. Figure 14a); HP3 is shown in van der Waals representation with blue carbons, while PP2 is shown in ball and stick representation with carbon atoms colored in orange. Dashed rings highlight the PP (green) and the Y (red) part of the PPXY recognition motif.

K give a good description of the folding landscape of the β-peptide hairpin HP2. Conformer C_{10} can be clearly identified as the native state at temperatures 300, 320, and 340 K (cf. Figure 14). The alternative conformers C_{12} and IM are approximately 4 kJ/mol less stable. This situation changes with the energy landscape at 370 K, where conformer C_{12} represents the native state. Conformers C_{10} and IM carry an energy penalty of about 2 and 8 kJ/mol, respectively.

Recognition of Proline-Rich Sequences (PRS). In the preceding parts, we have shown the strong tendency of rationally designed β-peptides to adopt hairpin-like conformations in water. This makes them extremely interesting as scaffolds for the design of molecules of pharmacological interest. An interesting example is the use of the introduced β-peptide hairpins to specifically tackle protein−protein interactions in cell signaling. In particular, we focus on PRS recognition in signal transduction. Most former attempts to tackle the recognition of PRS were based on the design of high affinity ligands, namely, improved polyproline peptides,[92–94] mini-proteins[95–97] or mimics.[98,99] We intend to provide a novel approach to mimic the receptor side, namely, the WW domain. This is the smallest of the proline-recognizing domains and thus a good starting point for the design of artificial PRS receptors. As already pointed out, a reduction of the PRS recognition site of the YAP65-WW domain to a β-hairpin mimicking the strands 2 and 3 should fulfill the needs for ligand binding.[54,59–61] Employing our rationally designed β-peptide scaffold, we circumvent the obvious peculiarities connected with α-peptides. On the basis of the interactions between the YAP65 WW domain strands 2 and 3 and its ligand PP2 (highest probability structure from the NMR ensemble 1JMQ[60]), we modified side A of HP2 with functionalities that enable the mimicry of these interactions and thus the binding of PP2 (Table 1). The A-side of the resulting peptide HP3 (Figure 2) resembles the PRS binding site of the YAP65 WW domain (Figure 15). The Trp side chains of residues BWY2 and BAW10 and the Tyr side chain of residue BRY9 form the hydrophobic patch for the recognition of the polyproline II structure of the PPXY target sequence. Additionally, the imino-function of the Trp side chain of residue BWY2 can satisfy a backbone carboxy function of PP2. Hydroxy and amino functions of B2I3 and BLK8 of HP3 resemble Thr37 and Lys30 of the YAP65-WW domain, respectively. The Tyr side chain of the peptide PP2 can interact with the aliphatic part of the Lys side chain of residue BLK8 and a H-bond between the hydroxy-functions of Tyr and the His side chain of residue BQH7 further stabilize this complex.

We manually superimposed the scaffold HP3 with the reduced WW domain (Figure 15) to estimate the correct orientation of PP2 relative to HP3 and obtain the starting conformation for the simulation of the complex. The HP3/PP2 complex remains stable in a 10 ns MD simulation. The highest populated cluster 5 includes 92% of the conformations from the 10 ns trajectory and is present during the whole simulation time (Figure 16a). The remaining 8% of possible conformations spread to 131 clusters. The clustering is performed by first fitting all structures to the backbone of the receptor HP3 and then clustering the heavy atoms of the sequence P^4PPY^7 with a 0.1 nm cutoff. In Figure 16b, the rmsd of the recognition sequence PPXY after fitting the whole complex to the HP3 backbone is shown for the 10 ns simulation time. Between 8 to 9 ns simulation time, a rarely populated alternative appears, which is apparent from the plots in Figure 16a,b. The stability of the complex and the specific interactions established by PP2 and HP3 make us propose β-peptide hairpins as promising mimics of PRS binding domains.

Conclusion

In this study, we present the first REMD study on the folding behavior of β-peptides in water. Despite some shortcomings of the REMD technique, as for instance differing exchange probabilities depending on the system sizes, REMD has proved to be a valuable tool to study the folding behavior and conformational space of peptides.

We show that β-peptide hairpins possess an enormous potential for the design of small receptors and binders of sequence motifs of proteins. They exhibit a nature-like folding behavior and combine robust structure formation and a putatively better bioavailability. Besides, the possibility of the positioning of a wide variety of functions on one side of this scaffold, which is only limited by synthetic availability, is rather tempting for several purposes. A demand for the design of small receptors from non-natural peptides is their stability in water, which we have clearly shown for our systems. The designed β-peptide hairpins outperform α-peptides in terms of folding toward hairpin-like structures. The estimated Gibbs free energy landscapes of HP2 have shown their interesting folding behavior, like the transition from conformer C_{10} to C_{12}. These properties will attract our interest in upcoming studies. We have proven their qualification as a scaffold for peptide design by the transfer of the side chains necessary for the binding of the WW domain to a PRS.

There are still ways to further stabilize our β-peptide hairpins; the exchange of the turn motif BGV-BKG to a more rigid scaffold could possibly further improve the folding properties. In taking into account the strong tendency of heterochiral $\beta^{2,3}$-amino acids to the formation of extended and strand-like conformations, an interesting idea to pursue would be to use both sides to develop a "hook-and-loop" fastener in order to connect two proteins with incompatible interfaces.

Acknowledgment. The authors thank Xavier Daura and David van der Spoel for support with the β-amino acid topologies for the Gromos force field, Hans-Jörg Hofmann and Fernando Lopez-Ortiz for helpful discussion, and Gerd Anders for scripting. MD simulations were performed at the Center for High Performance Computing (ZIH) of the TU Dresden. This work has been funded by the Free State of Saxony and the Klaus Tschira Stiftung gGmbH.

References and Notes

(1) Gellman, S. H. *Acc. Chem. Res.* **1998**, *31*, 173.
(2) Andrews, M. J. I.; Tabor, A. B. *Tetrahedron* **1999**, *55*, 11711.
(3) Kirshenbaum, K.; Zuckermann, R. N.; Dill, K. A. *Curr. Opin. Struct. Biol.* **1999**, *9*, 530.
(4) Koert, U. *Angew. Chem.* **1997**, *109*, 1922.
(5) North, M. *J. Pept. Sci.* **2000**, *6*, 301.
(6) Palomo, C.; Aizpurua, J. M.; Ganboa, I.; Oiarbide, M. *Amino Acids* **1999**, *16*, 321.
(7) Seebach, D.; Matthews, J. L. *J. Chem. Soc., Chem. Commun.* **1997**, *21*, 2015.
(8) Stigers, K. D.; Soth, M. J.; Nowick, J. S. *Curr. Opin. Chem. Biol.* **1999**, *3*, 714.
(9) Hill, D. J.; Mio, M. J.; Prince, R. B.; Hughes, T. S.; Moore, J. S. *Chem. Rev.* **2001**, *101*, 3893.
(10) Barron, A. E.; Zuckermann, R. N. *Curr. Opin. Chem. Biol.* **1999**, *3*, 681.
(11) Seebach, D.; Kimmerlin, T.; Sebesta, R.; Campo, M. A.; Beck, A. K. *Tetrahedron* **2004**, *60*, 7455.
(12) Möhle, K.; Günther, R.; Thormann, M.; Sewald, N.; Hofmann, H.-J. *Biopolymers* **1999**, *50*, 167.

(13) Günther, R.; Hofmann, H.-J. *Helv. Chim. Acta* **2002**, *85*, 2149.
(14) Baldauf, C.; Günther, R.; Hofmann, H.-J. *Angew. Chem., Int. Ed.* **2004**, *43*, 1594.
(15) Baldauf, C.; Günther, R.; Hofmann, H.-J. *Helv. Chim. Acta* **2003**, *86*, 2573.
(16) Baldauf, C.; Günther, R.; Hofmann, H.-J. *J. Org. Chem.* **2004**, *69*, 6214.
(17) Baldauf, C.; Günther, R.; Hofmann, H.-J. *J. Org. Chem.* **2005**, *70*, 5351.
(18) Schmitt, M. A.; Weisblum, B.; Gellman, S. H. *J. Am. Chem. Soc.* **2004**, *126*, 6848.
(19) Roy, R. S.; Karle, I. L.; Raghothama, S.; Balaram, P. *Proc. Natl. Acad. Sci. U.S.A.* **2004**, *101*, 16478.
(20) Hayen, A.; Schmitt, M. A.; Ngassa, F. N.; Thomasson, K. A.; Gellman, S. H. *Angew. Chem., Int. Ed.* **2004**, *43*, 505.
(21) De Pol, S.; Zorn, C.; Klein, C. D.; Zerbe, O.; Reiser, O. *Angew. Chem., Int. Ed.* **2004**, *43*, 511.
(22) Baldauf, C.; Günther, R.; Hofmann, H.-J. *Biopolymers* **2006**, *84*, 408.
(23) Baldauf, C.; Günther, R.; Hofmann, H.-J. *J. Org. Chem.* **2006**, *71*, 1200.
(24) Ananda, K.; Vasudev, P. G.; Sengupta, A.; Raja, K. M. P.; Shamala, N.; Balaram, P. *J. Am. Chem. Soc.* **2005**, *127*, 16668.
(25) Hintermann, T.; Seebach, D. *Chimia* **1997**, *51*, 244.
(26) Seebach, D.; Beck, A. K.; Bierbaum, D. J. *Chem. & Biodiv.* **2004**, *1*, 1111.
(27) Goodman, C. M.; Choi, S.; Shandler, S.; DeGrado, W. F. *Nat. Chem. Biol.* **2007**, *3*, 252.
(28) Dado, G. P.; Gellman, S. H. *J. Am. Chem. Soc.* **1994**, *116*, 1054.
(29) Appella, D. H.; Christianson, L. A.; Karle, I. L.; Powell, D. R.; Gellman, S. H. *J. Am. Chem. Soc.* **1996**, *118*, 13071.
(30) Seebach, D.; Overhand, M.; Kühnle, F. N. M.; Martinoni, B.; Oberer, L.; Hommel, U.; Widmer, H. *Helv. Chim. Acta* **1996**, *79*, 913.
(31) Seebach, D.; Ciceri, P. E.; Overhand, M.; Jaun, B.; Rigo, D.; Oberer, L.; Hommel, U.; Amstutz, R.; Widmer, H. *Helv. Chim. Acta* **1996**, *79*, 2043.
(32) Günther, R.; Hofmann, H.-J.; Kuczera, K. *J. Phys. Chem. B* **2001**, *105*, 5559.
(33) Appella, D. H.; Christianson, L. A.; Klein, D. A.; Powell, D. R.; Huang, X.; Barchi, J., Jr.; Gellman, S. H. *Nature (London)* **1997**, *387*, 381.
(34) De Ilarduya, A. M.; Alemán, C.; García-Alvarez, M.; López-Carrasquero, F.; Muñoz-Guerra, S. *Macromolecules* **1999**, *32*, 3257.
(35) DeGrado, W. F.; Schneider, J. P.; Hamuro, Y. *J. Pept. Res.* **1999**, *54*, 206.
(36) Gademann, K.; Hintermann, T.; Schreiber, J. *Curr. Med. Chem.* **1999**, *6*, 905.
(37) García-Alvarez, M.; León, S.; Alemán, C.; Campos, J. L.; Muñoz-Guerra, S. *Macromolecules* **1998**, *31*, 124.
(38) Wang, X.; Espinosa, J. F.; Gellman, S. H. *J. Am. Chem. Soc.* **2000**, *122*, 4821.
(39) Wu, Y.-D.; Wang, D.-P. *J. Am. Chem. Soc.* **1999**, *121*, 9352.
(40) Rueping, M.; Schreiber, J. V.; Lelais, G.; Jaun, B.; Seebach, D. *Helv. Chim. Acta* **2002**, *85*, 2577.
(41) Gademann, K.; Hane, A.; Rueping, M.; Jaun, B.; Seebach, D. *Angew. Chem., Int. Ed.* **2003**, *42*, 1534.
(42) Baldauf, C.; Günther, R.; Hofmann, H.-J. *Phys. Biol.* **2006**, *3*, S1.
(43) Hamuro, Y.; Schneider, J. P.; DeGrado, W. F. *J. Am. Chem. Soc.* **1999**, *121*, 12200.
(44) Schmitt, M. A.; Weisblum, B.; Gellman, S. H. *J. Am. Chem. Soc.* **2007**, *129*, 417.
(45) Epand, R. F.; Schmitt, M. A.; Gellman, S. H.; Epand, R. M. *Biochim. Biophys. Acta-Biomembr.* **2006**, *1758*, 1343.
(46) English, E. P.; Chumanov, R. S.; Gellman, S. H.; Compton, T. *J. Biol. Chem.* **2006**, *281*, 2661.
(47) Epand, R. F.; Schmitt, M. A.; Gellman, S. H.; Sen, A.; Auger, M.; Hughes, D. W.; Epand, R. M. *Mol. Membr. Biol.* **2005**, *22*, 457.
(48) Stephens, O. M.; Kim, S.; Welch, B. D.; Hodsdon, M. E.; Kay, M. S.; Schepartz, A. *J. Am. Chem. Soc.* **2005**, *127*, 13126.
(49) Kritzer, J. A.; Hodsdon, M. E.; Schepartz, A. *J. Am. Chem. Soc.* **2005**, *127*, 4118.
(50) Kritzer, J. A.; Stephens, O. M.; Guarracino, D. A.; Reznik, S. K.; Schepartz, A. *Bioorg. Med. Chem.* **2005**, *13*, 11.
(51) Kritzer, J. A.; Lear, J. D.; Hodsdon, M. E.; Schepartz, A. *J. Am. Chem. Soc.* **2004**, *126*, 9468.
(52) Sadowsky, J. D.; Fairlie, W. D.; Hadley, E. B.; Lee, H. S.; Umezawa, N.; Nikolovska-Coleska, Z.; Wang, S. M.; Huang, D. C. S.; Tomita, Y.; Gellman, S. H. *J. Am. Chem. Soc.* **2007**, *129*, 139.
(53) Sadowsky, J. D.; Schmitt, M. A.; Lee, H. S.; Umezawa, N.; Wang, S. M.; Tomita, Y.; Gellman, S. H. *J. Am. Chem. Soc.* **2005**, *127*, 11966.
(54) Kay, B. K.; Williamson, M. P.; Sudol, P. *Faseb Journal* **2000**, *14*, 231.
(55) Sudol, M.; Hunter, T. *Cell* **2000**, *103*, 1001.
(56) Sudol, M. *Trends Biochem. Sci.* **1996**, *21*, 161.
(57) Sudol, M. *Exp. Mol. Med.* **1996**, *28*, 65.
(58) Macias, M. J.; Wiesner, S.; Sudol, M. *FEBS Lett.* **2002**, *513*, 30.
(59) Macias, M. J.; Hyvonen, M.; Baraldi, E.; Schultz, J.; Sudol, M.; Saraste, M.; Oschkinat, H. *Nature* **1996**, *382*, 646.
(60) Pires, J. R.; Taha-Nejad, F.; Toepert, F.; Ast, T.; Hoffmuller, U.; Schneider-Mergener, J.; Kuhne, R.; Macias, M. J.; Oschkinat, L. *J. Mol. Biol.* **2001**, *314*, 1147.
(61) Espinosa, J. F.; Syud, F. A.; Gellman, S. H. *Biopolymers* **2005**, *80*, 303.
(62) Fisk, J. D.; Gellman, S. H. *J. Am. Chem. Soc.* **2001**, *123*, 343.
(63) Gellman, S. H. *Curr. Opin. Chem. Biol.* **1998**, *2*, 717.
(64) Giannis, A.; Kolter, T. *Angew. Chem., Int. Ed.* **1993**, *32*, 1244.
(65) Daura, X.; Gademann, K.; Schafer, H.; Jaun, B.; Seebach, D.; van Gunsteren, W. F. *J. Am. Chem. Soc.* **2001**, *123*, 2393.
(66) Lin, J. Q.; Luo, S. W.; Wu, Y. D. *J. Comput. Chem.* **2002**, *23*, 1551.
(67) Beke, T.; Csizmadia, I. G.; Perczel, A. *J. Am. Chem. Soc.* **2006**, *128*, 5158.
(68) Zeng, J. *Comb. Chem. High Throughput Screen.* **2000**, *3*, 355.
(69) Hukushima, K.; Nemoto, K. *J. Phys. Soc. Jpn.* **1996**, *65*, 1604.
(70) Sugita, Y.; Okamoto, Y. *Chem. Phys. Lett.* **1999**, *314*, 141.
(71) Okabe, T.; Kawata, M.; Okamoto, Y.; Mikami, M. *Chem. Phys. Lett.* **2001**, *335*, 435.
(72) Seibert, M. M.; Patriksson, A.; Hess, B.; van der Spoel, D. *J. Mol. Biol.* **2005**, *354*, 173.
(73) Cochran, A. G.; Skelton, N. J.; Starovasnik, M. A. *Proc. Natl. Acad. Sci. U.S.A.* **2001**, *98*, 5578.
(74) Cochran, A. G.; Skelton, N. J.; Starovasnik, M. A. *Proc. Natl. Acad. Sci. U.S.A.* **2002**, *99*, 9081.
(75) Zhang, J.; Qin, M.; Wang, W. *Proteins: Struct., Funct., Bioinformatics* **2006**, *62*, 672.
(76) Lindahl, E.; Hess, B.; van der Spoel, D. *J. Mol. Model.* **2001**, *7*, 306.
(77) Van der Spoel, D.; Lindahl, E.; Hess, B.; Groenhof, G.; Mark, A. E.; Berendsen, H. J. C. *J. Comput. Chem.* **2005**, *26*, 1701.
(78) Oostenbrink, C.; Soares, T. A.; van der Vegt, N. F. A.; van Gunsteren, W. F. *Eur. Biophys. J. Biophys. Lett.* **2005**, *34*, 273.
(79) Oostenbrink, C.; Villa, A.; Mark, A. E.; Van Gunsteren, W. F. *J. Comput. Chem.* **2004**, *25*, 1656.
(80) Daura, X.; van Gunsteren, W. F.; Rigo, D.; Jaun, B.; Seebach, D. *Chem. Eur. J.* **1997**, *3*, 1410.
(81) Daura, X.; Gademann, K.; Jaun, B.; Seebach, D.; van Gunsteren, W. F.; Mark, A. E. *Angew. Chem., Int. Ed.* **1999**, *38*, 236.
(82) Daura, X.; van Gunsteren, W. F.; Mark, A. E. *Proteins: Struct., Funct., Genetics* **1999**, *34*, 269.
(83) Trzesniak, D.; Jaun, B.; Mathad, R. I.; van Gunsteren, W. F. *Biopolymers* **2006**, *83*, 636.
(84) Humphrey, W.; Dalke, A.; Schulten, K. *J. Mol. Graph.* **1996**, *14*, 33.
(85) Berendsen, H. J. C.; Postma, J. P. M.; van Gunsteren, W. F.; DiNola, A.; Haak, J. R. *J. Chem. Phys.* **1984**, *81*, 3684.
(86) Miyamoto, S.; Kollman, P. A. *J. Comput. Chem.* **1992**, *13*, 952.
(87) Essmann, U.; Perera, L.; Berkowitz, M. L.; Darden, T.; Lee, H.; Pedersen, L. G. *J. Chem. Phys.* **1995**, *103*, 8577.
(88) Hess, B.; Bekker, H.; Berendsen, H. J. C.; Fraaije, J. *J. Comput. Chem.* **1997**, *18*, 1463.
(89) Appella, D. H.; Christianson, L. A.; Karle, I. L.; Powell, D. R.; Gellman, S. H. *J. Am. Chem. Soc.* **1999**, *121*, 6206.
(90) Appella, D. H.; Christianson, L. A.; Klein, D. A.; Richards, M. R.; Powell, D. R.; Gellman, S. H. *J. Am. Chem. Soc.* **1999**, *121*, 7574.
(91) Hofmann, H.-J., personal communication, unpublished results.
(92) Pisabarro, M. T.; Serrano, L.; Wilmanns, M. *J. Mol. Biol.* **1998**, *281*, 513.
(93) Wittekind, M.; Mapelli, C.; Lee, V.; Goldfarb, V.; Friedrichs, M. S.; Meyers, C. A.; Mueller, L. *J. Mol. Biol.* **1997**, *267*, 933.
(94) Pisabarro, M. T.; Serrano, L. *Biochemistry* **1996**, *35*, 10634.
(95) Golemi-Kotra, D.; Mahaffy, R.; Footer, M. J.; Holtzman, J. H.; Pollard, T. D.; Theriot, J. A.; Schepartz, A. *J. Am. Chem. Soc.* **2004**, *126*, 4.
(96) Chin, J. W.; Schepartz, A. *J. Am. Chem. Soc.* **2001**, *123*, 2929.
(97) Cobos, E. S.; Pisabarro, M. T.; Vega, M. C.; Lacroix, E.; Serrano, L.; Ruiz-Sanz, J.; Martinez, J. C. *J. Mol. Biol.* **2004**, *342*, 355.
(98) Jacquot, Y.; Broutin, I.; Miclet, E.; Nicaise, M.; Lequin, O.; Goasdoue, N.; Joss, C.; Karoyan, P.; Desmadril, M.; Ducruix, A.; Lavielle, S. *Bioorg. Med. Chem.* **2007**, *15*, 1439.
(99) Vidal, M.; Liu, W. Q.; Lenoir, C.; Salzmann, J.; Gresh, N.; Garbay, C. *Biochemistry* **2004**, *43*, 7336.

JP076838R